NATIONAL ADVISORY COMMITTEE FOR AERONAUTICS

TECHNICAL NOTE

No. 1064

LIFTING-SURFACE-THEORY RESULTS FOR THIN ELLIPTIC WINGS OF ASPECT RATIO 3 WITH CHORDWISE LOADINGS CORRESPONDING TO 0.5-CHORD PLAIN FLAP AND TO PARABOLIC-ARC CAMBER

By Stewart M. Crandall

Langley Memorial Aeronautical Laboratory
Langley Field, Va.

Washington
May 1946

NATIONAL ADVISORY COMMITTEE FOR AERONAUTICS

TECHNICAL NOTE NO. 1064

LIFTING-SURFACE-THEORY RESULTS FOR THIN ELLIPTIC WINGS OF ASPECT RATIO 3 WITH CHORDWISE LOADINGS CORRESPONDING TO 0.5-CHORD PLAIN FLAP AND TO PARABOLIC-ARC CAMBER

By Stewart M. Crandall

SUMMARY

As part of a general investigation of methods of calculating hinge-moment and lift characteristics of control surfaces on finite-span wings from two-dimensional data, the electromagnetic-analogy method was used to provide lifting-surface-theory solutions applicable to the determination of aspect-ratio corrections for the slope of the curve of hinge-moment coefficient against flap deflection. Solutions were obtained for two vortex patterns representing unswept elliptic wings having aspect ratios of 3. The chordwise loads corresponded to a thin airfoil with a 0.5-chord plain flap and to a thin airfoil with parabolic-arc camber, both in two-dimensional flow. The vertical component of the induced-velocity field of the two vortex patterns was determined; however, the actual method of applying the results to hinge-moment and lift computations is not discussed.

A comparison of the results of the present measurements with those of previous tests indicated that the increment of induced downwash at the 0.5-chord line over the value predicted by lifting-line theory is a linear function of the center-of-pressure coefficient. This increment decreases as the center of pressure moves toward the trailing edge of the airfoil. The induced camber decreases as the center of pressure of the two-dimensional load moves toward the leading edge. This variation does not appear to be linear.

INTRODUCTION

Lifting-line theory has proved inadequate for the computation of the hinge-moment characteristics of control

surfaces of finite-span wings from two-dimensional data. Lifting-surface-theory solutions for thin unswept elliptic wings at an angle of attack have been used in computing the slope of the curve of hinge-moment coefficient against angle of attack for small angles of attack (reference 1). The results were in good agreement with experiment.

A description of the electromagnetic-analogy method of solving lifting-surface-theory problems is presented in reference 2. Two electromagnetic-analogy models were constructed and tested to provide lifting-surface-theory solutions applicable to the determination of aspect-ratio corrections for the slope of the curve of hinge-moment coefficient against flap deflection. The models were elliptic in plan form and had an aspect ratio of 3. The chordwise loadings corresponded to a thin airfoil with a 0.5-chord plain flap and to a thin airfoil with parabolic-arc camber, both in two-dimensional flow. The present report gives the results of these tests and a comparison with values predicted on the basis of lifting-line theory.

SYMBOLS

Γ	circulation from leading edge to general point
c_l	section lift coefficient $\left(\frac{\text{Lift}}{qc}\right)$
α	angle of attack
α_o	angle of attack for infinite aspect ratio
δ	flap deflection
c_{l_α}	section slope of curve of lift coefficient with angle of attack $\left(\frac{\partial c_l}{\partial \alpha_o}\right)_\delta$
c_{l_δ}	section slope of curve of lift coefficient with flap deflection $\left(\frac{\partial c_l}{\partial \delta}\right)_{\alpha_o}$
$(\alpha_\delta)_{c_l}$	section lift effectiveness $\left(\left\lvert\left(\frac{\partial \alpha}{\partial \delta}\right)_{c_l}\right\rvert = \frac{c_{l_\delta}}{c_{l_\alpha}}\right)$
q	free-stream dynamic pressure $\left(\frac{1}{2}\rho V^2\right)$

ρ	fluid density
V	free-stream velocity
w	vertical component of induced velocity
b	wing span
S	wing area
A	aspect ratio (b^2/S)
c	wing chord
c_s	wing chord at plane of symmetry
c_f	flap chord
β	ratio of maximum ordinate of a thin parabolic-arc airfoil to its semichord $\left(\frac{z_{max}}{c/2}\right)$
z_{max}	maximum ordinate of thin parabolic-arc airfoil
C_p	center-of-pressure coefficient (ratio of distance of center of pressure from leading edge to chord)
x	chordwise distance from wing leading edge
y	spanwise distance from plane of symmetry
θ	parameter defining chordwise position $\left(\cos^{-1}\left(1 - \frac{x}{c/2}\right)\right)$
θ_f	parameter defining flap location $\left(\cos^{-1}\left(\frac{c_f}{c/2} - 1\right)\right)$

Subscripts:

LL	lifting-line theory
max	maximum
pa	parabolic-arc-camber chord loading
flap	flap chord loading

ELECTROMAGNETIC-ANALOGY MODELS

Vortex Patterns

In order to construct electromagnetic-analogy models of the wing with flap and the wing with parabolic-arc camber, the vortex patterns that are to represent the two wings and their wakes must first be determined. The load was assumed to be distributed chordwise according to thin-airfoil theory and spanwise in proportion to the chord.

Elliptic wing with 0.5-chord-flap chord loading.- The ratio of the circulation from the leading edge of the airfoil to a point x at any spanwise station to the total circulation from the leading edge to the trailing edge is given by the chordwise circulation function $2\Gamma/cc_l V$. From thin-airfoil theory the value of this function for a flat plate with a plain flap is

$$\left(\frac{2\Gamma}{cc_l V}\right)_{flap} = \frac{(\pi - \theta_f)(\theta + \sin\theta) + (\cos\theta - \cos\theta_f)\log_e\left|\frac{1 - \cos(\theta - \theta_f)}{\cos\theta - \cos\theta_f}\right| + \theta\sin\theta_f}{\pi(\pi - \theta_f + \sin\theta_f)} \tag{1}$$

This relation may be derived from the velocity-potential functions presented in reference 3 and is shown in figure 1 for a flap-chord ratio of 0.5.

The load per unit span $cc_l q$ at a general point y is given by

$$cc_l q = c(2\pi)(\alpha_\delta)_{c_l}\delta q$$

$$= c_s\sqrt{1 - \left(\frac{y}{b/2}\right)^2}\,(2\pi)(\alpha_\delta)_{c_l}\delta q$$

whence

$$\frac{cc_l}{c_s\delta} = 2\pi(\alpha_\delta)_{c_l}\sqrt{1 - \left(\frac{y}{b/2}\right)^2}$$

Contour lines of the product $2\Gamma/c_s V\delta$ of the spanwise loading function $cc_l/c_s\delta$ and the chordwise

circulation function $\left(\frac{2\Gamma}{cc_l V}\right)_{flap}$ determine the vortex pattern of the wing with flap. Figure 2 shows 10 of these contour lines in terms of the parameter $\frac{2\Gamma}{c_s V\delta}\Big/\left(\frac{2\Gamma}{c_s V\delta}\right)_{max}$ or Γ/Γ_{max}.

Elliptic wing with parabolic-arc-camber chord loading.- A thin airfoil with parabolic-arc camber at zero angle of attack has an elliptic chordwise pressure distribution. The chordwise circulation function for such a pressure distribution may be shown to be

$$\left(\frac{2\Gamma}{cc_l V}\right)_{pa} = \frac{1}{\pi}\left(\theta - \frac{1}{2}\sin 2\theta\right) \qquad (2)$$

A plot of the function is presented in figure 3.

The load per unit span $cc_l q$ at a general point y is given by

$$cc_l q = 2\pi c\beta q$$

$$= 2\pi c_s \sqrt{1 - \left(\frac{y}{b/2}\right)^2}\,\beta q$$

whence

$$\frac{cc_l}{c_s\beta} = 2\pi\sqrt{1 - \left(\frac{y}{b/2}\right)^2}$$

The vortex pattern of the wing with parabolic-arc-camber chord loading is determined by contour lines of the product $2\Gamma/c_s V\beta$ of the spanwise loading function $cc_l/c_s\beta$ and the chordwise circulation function $\left(\frac{2\Gamma}{cc_l V}\right)_{pa}$. Ten contour lines for the elliptic wing with parabolic-arc camber are presented in figure 4.

Construction of Electromagnetic-Analogy Models

In order to simplify construction, only one semispan of each wing was simulated. The models were constructed by fastening $\frac{1}{16}$-inch-thick aluminum and brass strips to sheets of plywood. The span of each model was 8.33 feet, which is considerably larger than the spans of previous electromagnetic-analogy models tested (references 2 and 4). A larger span was used to increase the accuracy of the simulation of the vortex sheet and of the measurement of the magnetic-field strength. Details of the construction and the method of introducing the current into the strips at the center section of the model are shown in figure 5. The lead-in wires at the center section were perpendicular to the plane of the simulated vortex sheet so that the current flowing through these wires would not induce downwash in that plane.

Downwash Measurements

The method employed in making the measurements of the vertical component of the magnetic field induced by the electromagnetic-analogy models is described in reference 2. Measurements of the magnetic-field strength at both the real and the reflection points were made because only one semispan of each wing was simulated. The induced downwash was determined from the sum of the two readings. The induced magnetic-field strength was measured at about 50 chordwise points for five vertical heights and 20 spanwise positions for both models. Curves were faired through the measured data and extrapolations to zero height were made for six or seven chordwise stations. The extrapolated values of magnetic-field strength were then converted to the nondimensional downwash $wb/2\Gamma_{max}$.

Corrections applied for the finite length of the trailing vortices were computed by assuming the loading to be a simple rectangular loading (see reference 2). Experience has shown that this approximation gives corrections of satisfactory accuracy.

PRESENTATION OF RESULTS

Elliptic Wing with 0.5-Chord-Flap Chord Loading

According to a combination of lifting-line theory and thin-airfoil theory, the nondimensional downwash $wb/2\Gamma_{max}$ for an elliptic wing with a chord loading corresponding to that of a 0.5-chord plain flap in two-dimensional flow is given by

$$\left(\frac{wb}{2\Gamma_{max}}\right)_{LL} = \frac{1}{4} \qquad (x/c < 0.5) \qquad (3a)$$

$$\left(\frac{wb}{2\Gamma_{max}}\right)_{LL} = \frac{1}{4} + \frac{A}{8(a_\delta)_{c_l}} \qquad (x/c > 0.5) \qquad (3b)$$

The term $\frac{1}{4}$ represents the downwash induced by the trailing vortices as computed by lifting-line theory. According to thin-airfoil theory the downwash induced by the bound vorticity is zero for all points ahead of the flap hinge line, where the slope of the surface is zero (equation (3a)). The second term of equation (3b) represents the downwash induced by the bound vorticity behind the flap hinge line, where the slope of the surface is δ. For an aspect ratio of 3 and a 0.5-chord flap, this term has a value of 0.459.

Values of the nondimensional downwash $wb/2\Gamma_{max}$ for the wing with flap chord loading, determined by the electromagnetic-analogy method, are presented in figure 6 as a function of chordwise location for various spanwise positions. The lifting-line-theory values predicted by equation (3) are included for comparison. These data are replotted in figure 7 with the lifting-line-theory values (equation (3)) subtracted. This operation removes the discontinuity of the flap hinge line.

Elliptic Wing with Parabolic-Arc-Camber Chord Loading

According to a combination of lifting-line theory and thin-airfoil theory, the nondimensional downwash $wb/2\Gamma_{max}$ for an elliptic wing with a chord loading corresponding to that of a thin parabolic-arc airfoil at zero angle of attack in two-dimensional flow is

$$\left(\frac{wb}{2\Gamma_{max}}\right)_{LL} = \frac{1}{4} + \frac{A}{2}\left(\frac{x}{c} - 0.5\right) \qquad (4)$$

The first term on the right-hand side of equation (4) represents the downwash induced by the trailing vortices as determined from lifting-line theory and the second, that induced by the bound vorticity according to thin-airfoil theory.

Measured values of the parameter $wb/2\Gamma_{max}$ are presented in figure 8. In order to give a better illustration of the induced camber, the lifting-line-theory values of the induced-downwash parameter (equation (4)) were subtracted from the measured values and the results were plotted against spanwise location for various chordwise stations in figure 9.

DISCUSSION OF RESULTS

Induced Angle of Attack

Lifting-surface-theory solutions of unswept elliptic wings show the induced camber to be approximately parabolic, since the chordwise variation of downwash is approximately linear (see figs. 6 and 8). Because the angle of attack of a thin airfoil of parabolic shape is given by the slope of the mean line at the 0.5-chord point (reference 4), the induced angle of attack at the 0.5-chord line of an unswept elliptic wing is a measure of the induced loading of angle-of-attack chord loading. This induced angle of attack is thus determined from the values of the downwash $wb/2\Gamma_{max}$ at the 0.5-chord point.

In figure 10 values of the induced downwash $wb/2\Gamma_{max}$ at the 0.5-chord line, reduced by the amount predicted on

the basis of lifting-line theory, are plotted against the center-of-pressure coefficient of the two-dimensional load. The value for the angle-of-attack chord loading was obtained from reference 2. The increment in induced downwash appears to be directly proportional to the location of the center of pressure; the increment decreases as the center of pressure moves toward the trailing edge of the airfoil.

Induced Camber

The induced camber or so-called streamline curvature (references 1 and 4) is extremely important in determining the aspect-ratio corrections to hinge moments. The induced camber results in an increment of elliptic chord loading, which causes large changes in the pressure distribution near the airfoil trailing edge.

The induced camber as measured by the parameter $\frac{\partial\left(\frac{wb}{2\Gamma_{max}}\right)}{\partial(x/c)}$ is presented in figure 11 for three types of chord loading. The data for the angle-of-attack chord loading are obtained from reference 2. The induced camber decreased at all spanwise stations as the center of pressure moved toward the leading edge of the airfoil; however, no simple relation for expressing the variation is apparent.

CONCLUSIONS

Surveys of the vertical component of the induced velocity field of two vortex patterns have been made by the electromagnetic-analogy method. The vortex patterns represented elliptic wings having aspect ratios of 3 and chordwise loads corresponding to a thin airfoil with a 0.5-chord flap and a thin airfoil with parabolic-arc camber, both in two-dimensional flow. A study of the results of the present measurements and those previously made of a vortex pattern representing a wing of the same plan form with an angle-of-attack chord loading indicated the following conclusions:

1. The increment of induced downwash at the 0.5-chord line above the value predicted by lifting-line theory is

a linear function of the center-of-pressure location; the increment decreases as the center of pressure moves toward the trailing edge of the airfoil.

2. The induced camber decreases as the center of pressure of the section load moves toward the leading edge. The variation does not appear to be linear.

Langley Memorial Aeronautical Laboratory
National Advisory Committee for Aeronautics
Langley Field, Va., November 23, 1945

REFERENCES

1. Swanson, Robert S., and Gillis, Clarence L.: Limitations of Lifting-Line Theory for Estimation of Aileron Hinge-Moment Characteristics. NACA CB No. 3L02, 1943.

2. Swanson, Robert S., and Crandall, Stewart M.: An Electromagnetic-Analogy Method of Solving Lifting-Surface-Theory Problems. NACA ARR No. L5D23, 1945.

3. Theodorsen, Theodore: General Theory of Aerodynamic Instability and the Mechanism of Flutter. NACA Rep. No. 496, 1935.

4. Swanson, Robert S., and Priddy, E. LaVerne: Lifting-Surface-Theory Values of the Damping in Roll and of the Parameter Used in Estimating Aileron Stick Forces. NACA ARR No. L5F23, 1945.

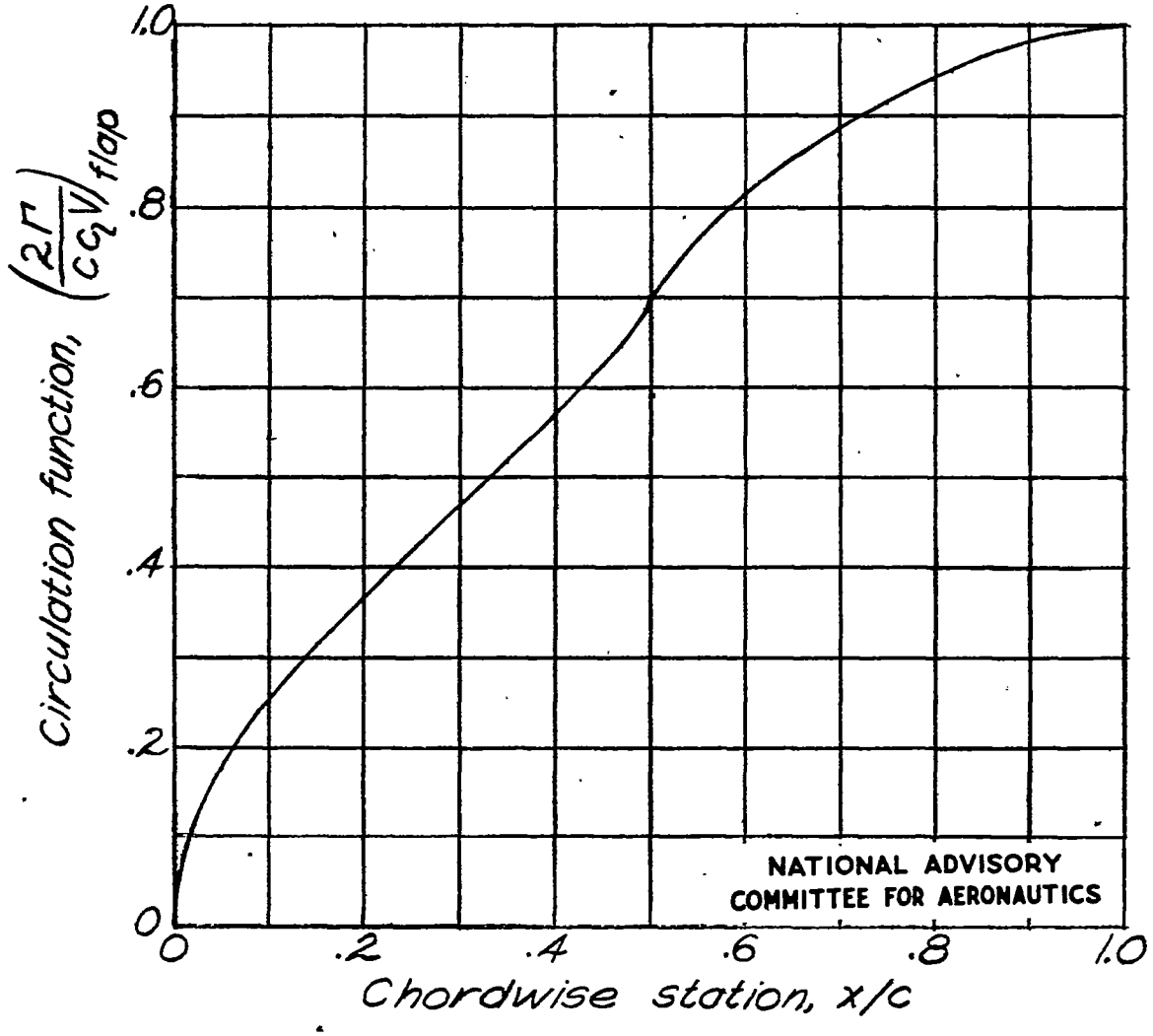

Figure 1.- Chordwise distribution of circulation function $(2\Gamma/cc_l V)_{flap}$ for a thin airfoil with a 0.5-chord flap. (Determined from thin-airfoil theory.)

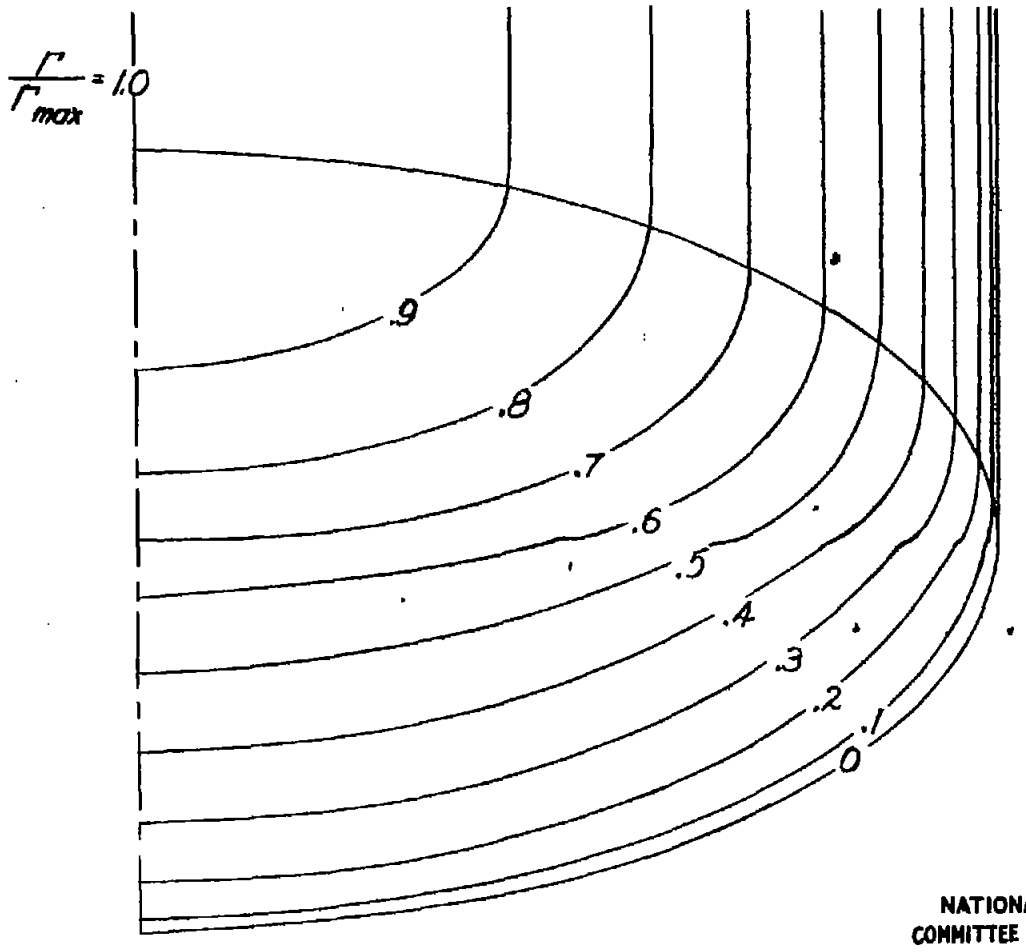

Figure 2.- Contour lines of the circulation function $\frac{2\Gamma}{c_s V6} \Big/ \left(\frac{2\Gamma}{c_s V6}\right)_{max}$ for an elliptic wing having an aspect ratio of 3 and 0.5-chord-flap chord loading.

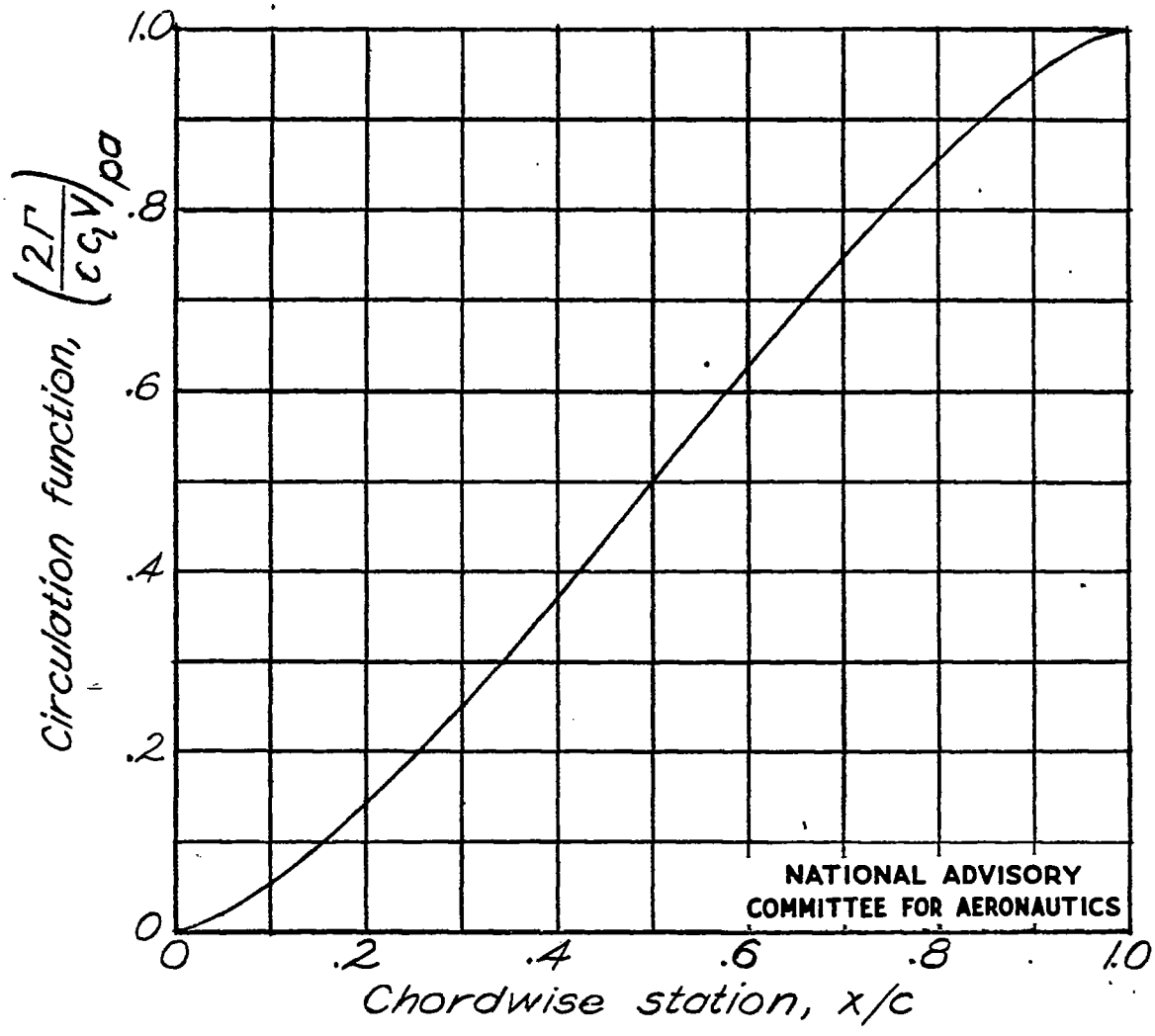

Figure 3.- Chordwise distribution of circulation function $(2\Gamma/cc_l V)_{pa}$ for a thin airfoil with parabolic-arc camber. (Determined from thin-airfoil theory.)

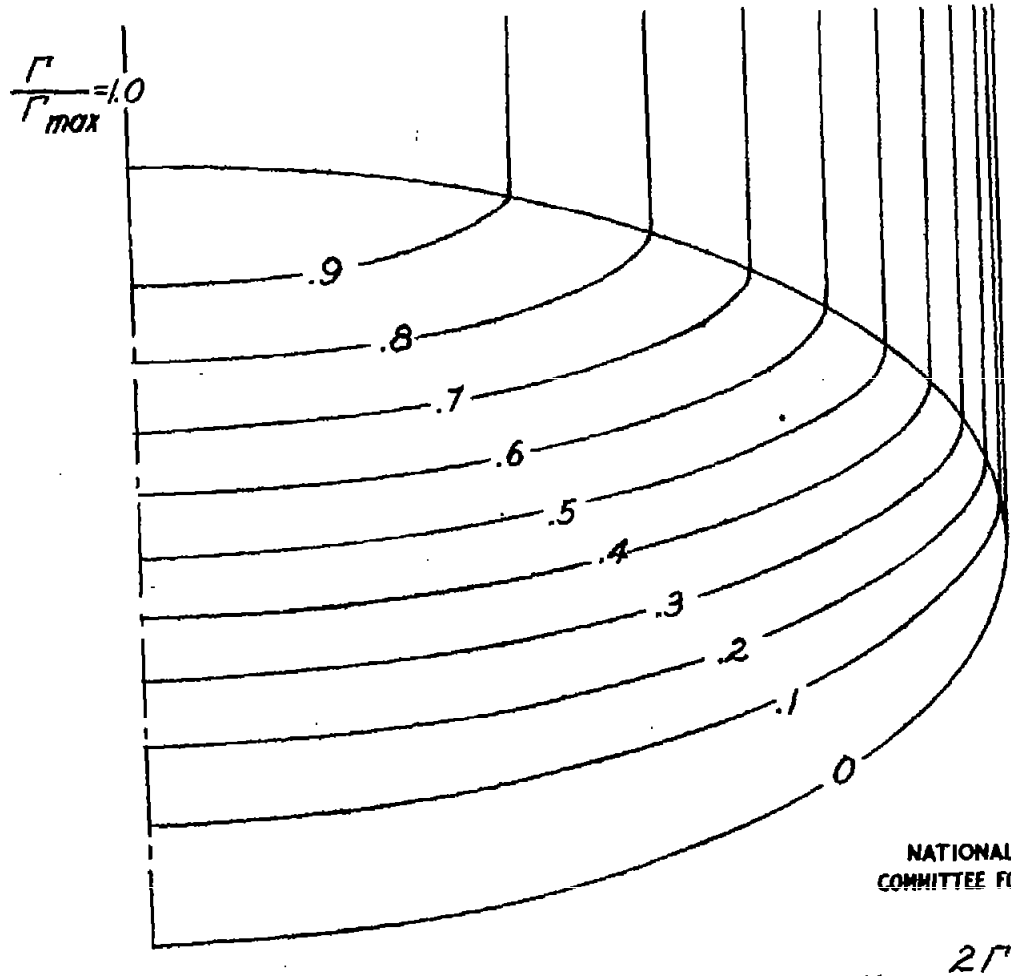

Figure 4.- Contour lines of the circulation function $\frac{2\Gamma}{c_s V\beta} \Big/ \left(\frac{2\Gamma}{c_s V\beta}\right)_{max}$ for an elliptic wing having an aspect ratio of 3 and parabolic-arc-camber chord loading.

Figure 5.- Electromagnetic-analogy model of an elliptic wing having an aspect ratio of 3 and parabolic-arc-camber chord loading.

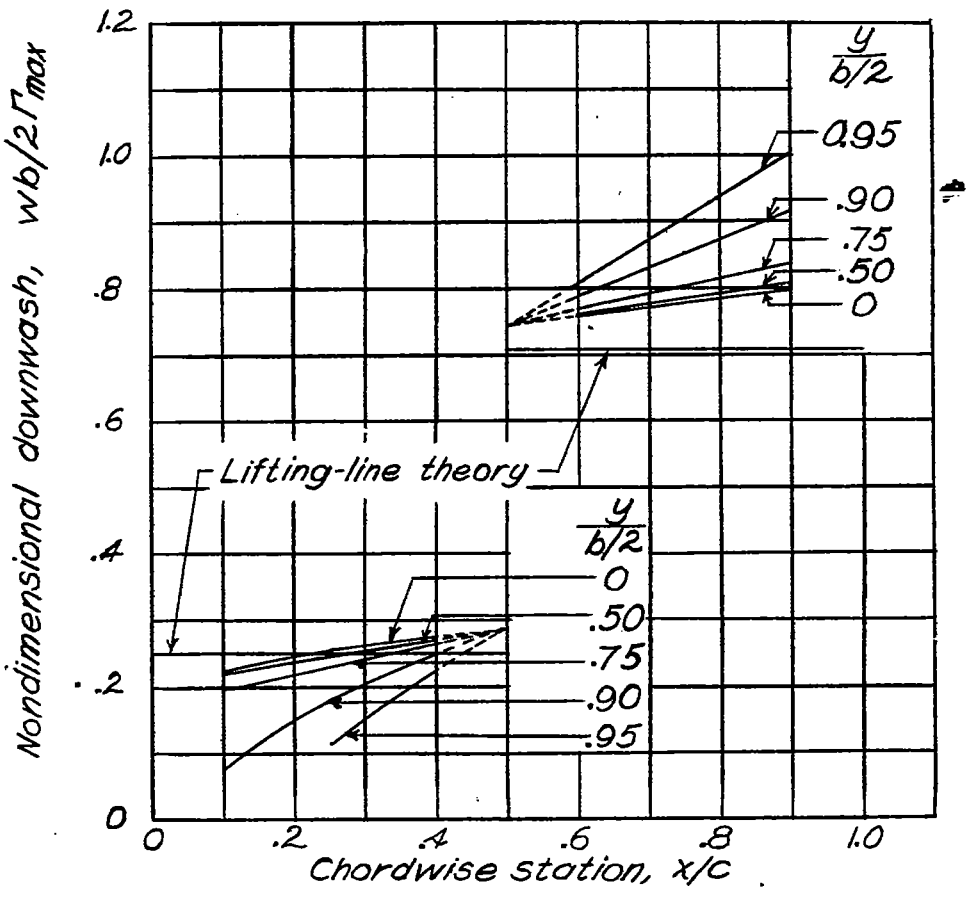

Figure 6.- The nondimensional downwash $\frac{wb}{2\Gamma_{max}}$ for a thin elliptic wing having an aspect ratio of 3 and 0.5-chord-flap chord loading. Values obtained from tests of an electromagnetic-analogy model.

NATIONAL ADVISORY
COMMITTEE FOR AERONAUTICS

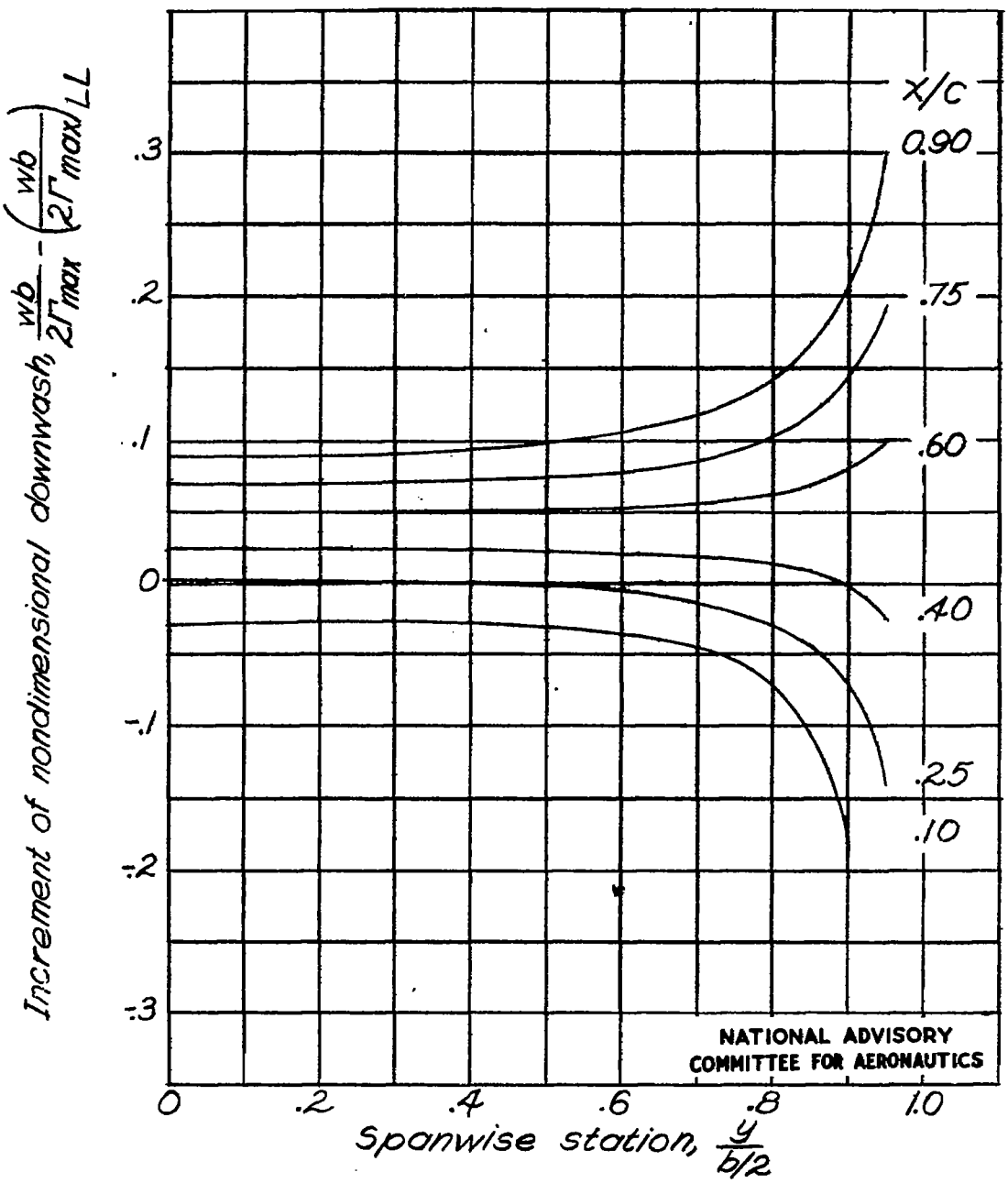

Figure 7.- The increment of nondimensional downwash $\frac{wb}{2\Gamma_{max}} - \left(\frac{wb}{2\Gamma_{max}}\right)_{LL}$ for an elliptic wing having an aspect ratio of 3 and 0.5-chord-flap chord loading. Values obtained from tests of an electromagnetic-analogy model.

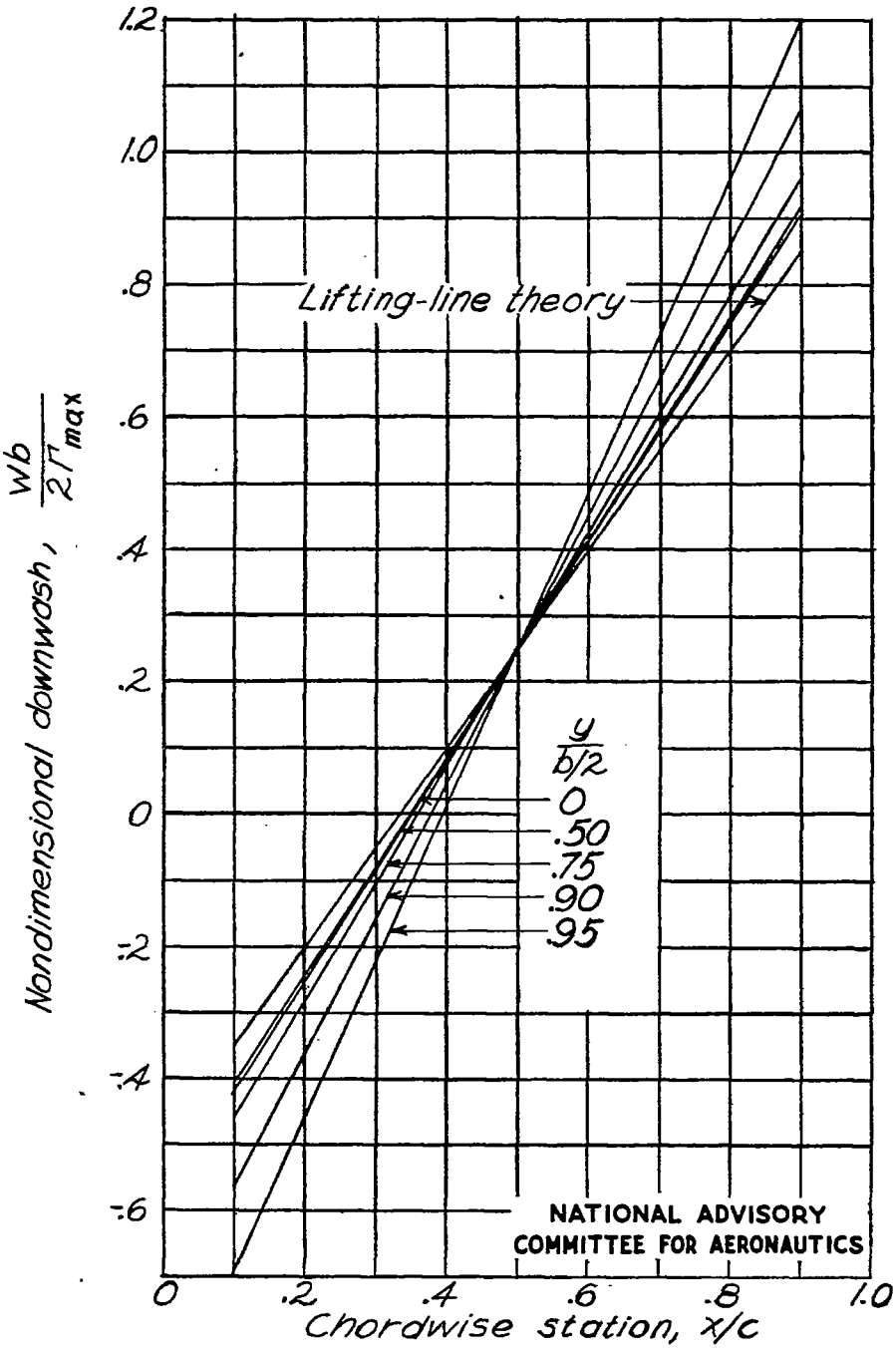

Figure 8.- The nondimensional downwash $wb/2\Gamma_{max}$ for a thin elliptic wing having an aspect ratio of 3 and parabolic-arc-camber chord loading. Values obtained from tests of an electromagnetic-analogy model.

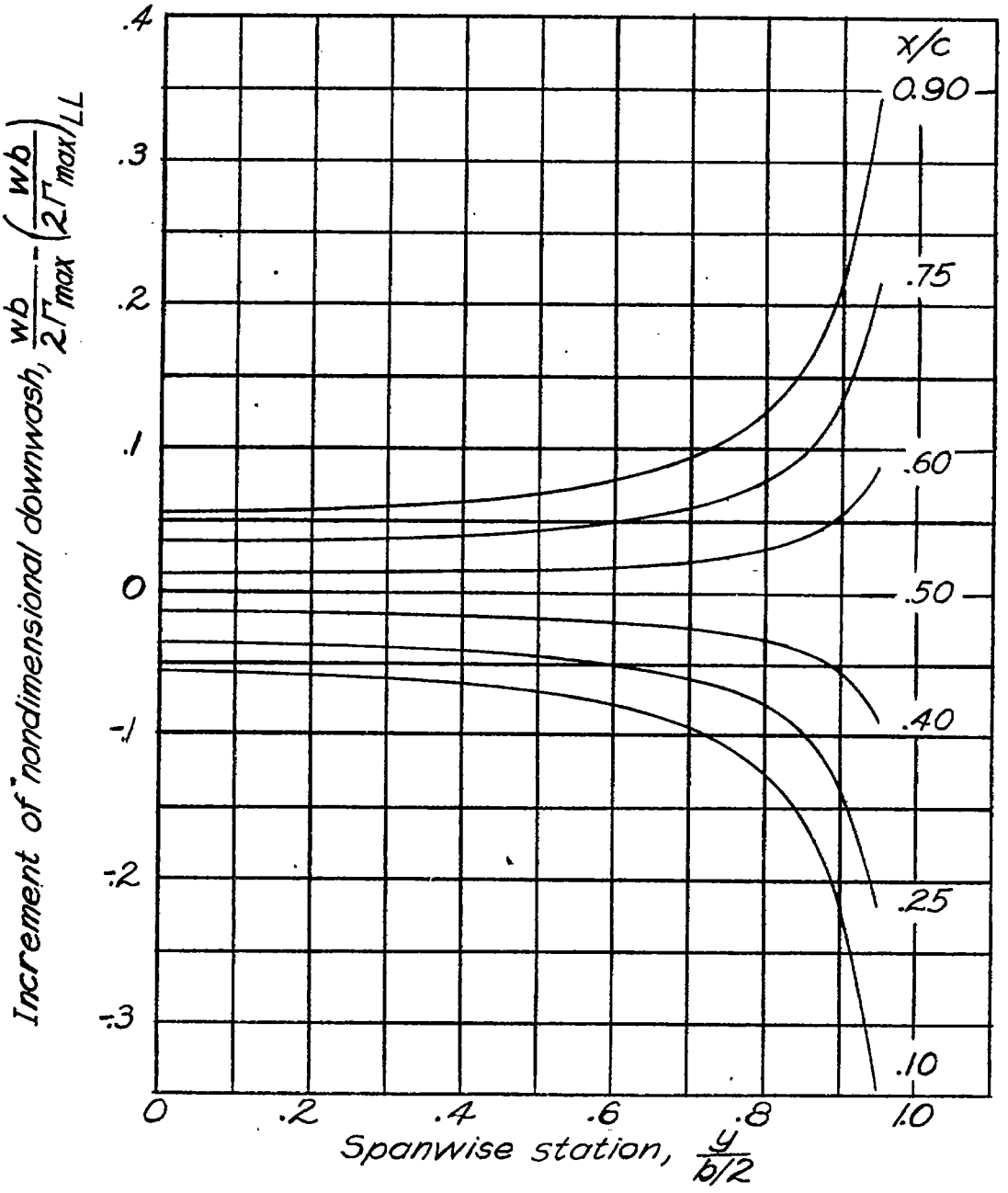

Figure 9.- The increment of nondimensional downwash $\frac{wb}{2\Gamma_{max}} - \left(\frac{wb}{2\Gamma_{max}}\right)_{LL}$ for an elliptic wing having an aspect ratio of 3 with parabolic-arc-camber chord loading. Values obtained from tests of an electromagnetic-analogy model.

NATIONAL ADVISORY
COMMITTEE FOR AERONAUTICS

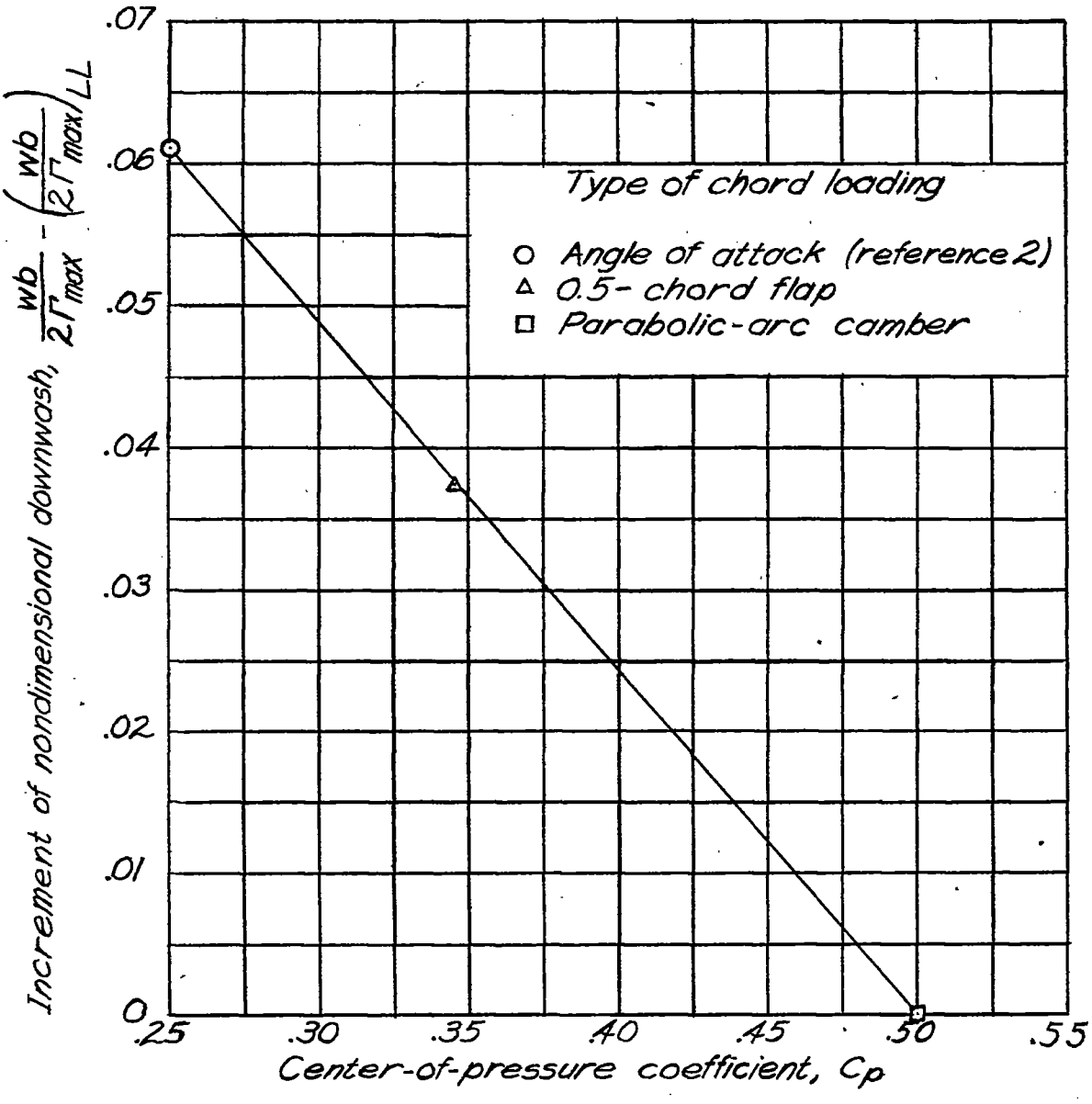

Figure 10- Increment of nondimensional downwash $\frac{wb}{2\Gamma_{max}} - \left(\frac{wb}{2\Gamma_{max}}\right)_{LL}$ at the 0.5-chord line as a function of the center-of-pressure coefficient of the section load. Elliptic wings; A=3.

NATIONAL ADVISORY
COMMITTEE FOR AERONAUTICS

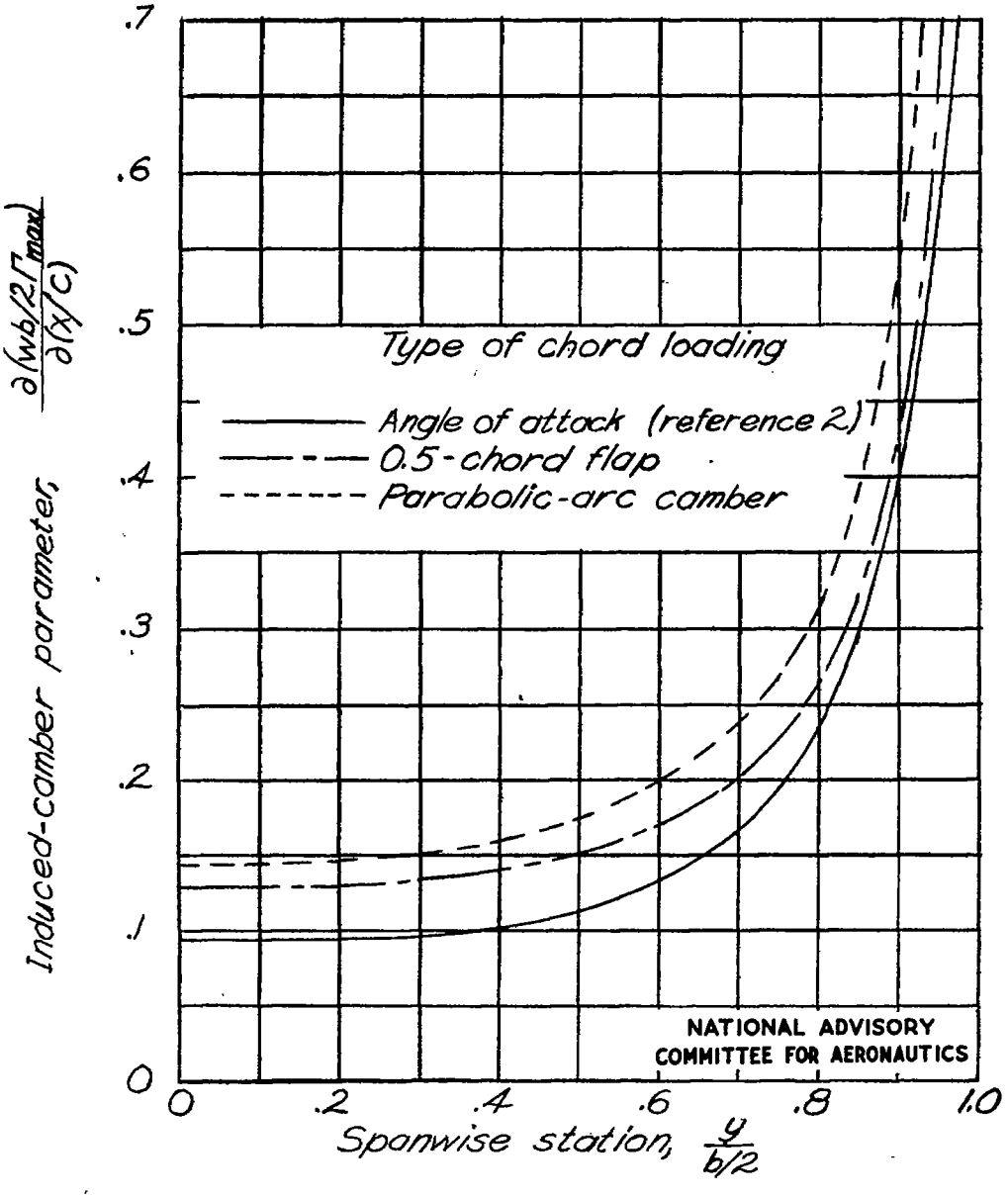

Figure 11. – Spanwise variation of the induced-camber parameter $\frac{\partial(wb/2\Gamma_{max})}{\partial(x/c)}$ for various chord loadings as determined by the electromagnetic-analogy method. Elliptic wings; A=3.